Supplemental Materials

Methods

Nanogel synthesis and characterization

Core-shell poly(N-isopropylacrylamide) p(NIPAM) nanogels were synthesized in two precipitation polymerization reactions. Nanogel cores were synthesized using 90% N-isopropylacrylamide (NIPAM) (Sigma-Aldrich) and 10% N,N'-methylenebis(acrylamide) (BIS) (Sigma-Aldrich) crosslinker at a total monomer concentration of 140mM. Monomer and crosslinker were dissolved in 99mL deionized water containing 2 mM sodium dodecyl sulfate (SDS) (Sigma-Aldrich). The solution was filtered through a 0.2 μm filter and heated to 70°C in a pre-heated oil bath at 450 rpm. With oxygen purging from the system with nitrogen gas, the reaction solution fluxed at 70°C for 1 hour, after which the reaction was initiated with 2 mM ammonium persulfate (APS) (Sigma-Aldrich) dissolved in 1mL deionized water and filtered through a 0.2 μm filter. The reaction continued for 6 hours at 70°C under a blanket of nitrogen at 450 rpm, after which the nanogel solution was cooled to room temperature, filtered through glass wood, and purified via dialysis using 1000kDa molecular weight cutoff dialysis tubing (Biotech CE Dialysis Tubing, Spectrum Laboratories) and dialyzing against deionized water twice and ultrapure water once over 72 hours. Nanogel shell addition involved a second precipitation polymerization reaction where a NIPAM-co-acrylic acid polymer was formed around nanogel cores. Here, 40 mL purified core nanogels were mixed with 60 mL of filtered monomer solution containing a total monomer concentration of 40mM with 93% NIPAM, 2% BIS, and 0.5 mM SDS. Again, the reaction was heated to 70°C in a pre-heated oil bath at 450 rpm with oxygen purged from the solution through nitrogen gas. After 50 minutes at 70°C, acrylic acid (AAc) (5% of total monomer concentration) was added to the reaction vessel. After 10 minutes, the reaction was

initiated with 1 mM APS in 1mL deionized water and filtered through a 0.2 μm filter. The reaction was carried out for 4 hours at 70°C under a blanket of nitrogen at 450 rpm, after which the reaction was cooled to room temperature overnight, filtered through glass wool, and purified via dialysis as previously mentioned. In studies where fluorescent particles were necessary, 0.1% methacryloxyethyl thiocarbamoyl rhodamine B monomer (Poly-science) was incorporated in the monomer solution during core nanogel synthesis.

Single layer nanogels were also synthesized for release studies comparison and were made in a precipitation polymerization reaction with 140mM total monomer concentration that contained 93% NIPAM, 2% BIS, and 5% AAc. Here, NIPAM monomer and BIS crosslinker were dissolved in 99 mL deionized water containing 3 mM sodium dodecyl sulfate (SDS) (Sigma-Aldrich). The solution was filtered through a 0.2 μm filter and heated to 70°C in a pre-heated oil bath at 450 rpm. With oxygen purging from the system with nitrogen gas, the reaction solution fluxed at 70°C for 50 minutes before adding AAc. After 10 more minutes, the reaction was initiated with 1mM APS dissolved in 1mL deionized water and filtered through a 0.2 μm filter. The reaction was carried out for 6 hours at 70°C under a blanket of nitrogen at 450 rpm, after which the reaction was cooled to room temperature overnight, filtered through glass wool, and purified via dialysis as previously mentioned. Lyophilization of particle was performed to resuspend at known concentrations.

Size characterization of particles types included particle tracking analysis with Malvern Nanosight to determine hydrodynamic diameter of individual particles under Brownian motion with the Stokes-Einstein equation. A minimum of 10^8 particles were analyzed per particle type. Atomic force microscopy (AFM) (Asylum Research MFP-3D) was utilized to determine dry particle diameter and height of nanogels on a glass surface. Coverslips were cleaned through 10-minute sonication periods in solutions of alconox, water, acetone, absolute ethanol, and then

isopropyl alcohol. Once dry, nanogel solutions were placed on the cleaned coverslips and allowed to dry again overnight before adhering to a glass microscope slide using cyanoacrylate and imaged using AFM. At least 30 particles were measured for each particle type. Additionally, SEM (JEOL JSM-7600F) was utilized to validate particle architecture. Here, coverslips were cleaned using the same procedure mentioned above and then treated with (3-aminopropyl)triethoxysilane (APTMS) (Sigma-Aldrich) for 2 hours and washed with deionized water. Nanogel solutions were placed over coverslips and centrifuged for 10 minutes at 3700 rpm. Then, nanogel solutions were removed, coverslips washed with deionized water, and dried. Coverslips were then sputter coated prior to SEM imaging.

Absorbance-based clotting analysis with tPA-loaded fibrin-specific nanogels

To test tissue-type plasminogen activator (tPA) released from FSNs, an endogenous fibrinolysis absorbance-based clotting assay was conducted. 90 μL fibrin clots were formed in HEPES buffer with 1mg/mL fibrinogen (Enzyme Research Laboratories), 10.8 μg/mL human plasminogen (Thermo Fisher Scientific), and 2 mg/mL tPA-FSNs or FSNs. Baseline absorbance values were recorded at 350 nm and then 10 μL of thrombin solution or water (no thrombin control) was added for a final concentration of 0.25 U/mL human alpha-thrombin (Fisher Scientific). The polymerizing fibrin clot was examined by monitoring clot absorbance at 350 nm every 30 seconds using a plate reader. Three clots were observed per condition.

In vitro fluidic device evaluation of clotting dynamics under active coagulation

Molds for the polydimethylsiloxane (PDMS) were modeled in SolidWorks and created with laser cut acrylic. A 10:1 ratio of silicone elastomer base to curing agent was used to fill molds. Once removed, PDMS devices were biopsy punched to allow for inlet and outlet polyurethane tubing and an opening at the clot reservoir. A glass slide was plasma treated and bound to the

fluidic device. A stationary fibrin clot boundary was formed in the clot reservoir with 2.5 mg/mL fibrinogen and 0.5 U/mL thrombin in HEPES buffer. 0.1 mg/mL Alexa-Fluor 488 labeled fibrinogen (Thermo Fisher Scientific) was used for visualization. The stationary clot was allowed to polymerize for at least 3 hours. Then, a syringe pump was connected to the inlet and an actively polymerizing solution was flowed into the device at a wall shear rate of 1 s^{-1}. After the solution passed the stationary clot boundary site, the experiment continued for 20 minutes. Solutions of 2.5 mg/mL fibrinogen, 0.1 U/mL thrombin, and +/- 10.8 μg/mL plasminogen acted as controls (n=7). 1 mg/mL nanogels were added in experimental conditions (FSNs (n=4), FSNs without thrombin (n=3), non-binding core-shell nanogels (n=3), tPA-loaded FSNs (n=4), tPA-loaded non-binding core-shell nanogels (n=3), and tPA-loaded CS-IgGs (n=3)). tPA alone conditions (n=3) included doses that were previously established from release studies from the same nanogel formulation. Rhodamine particles were utilized in all experiments and 0.05 mg/mL Alexa-Fluor 488 labeled fibrinogen was utilized for visualization. Images (4x magnification) were taken on an EVOS FL Auto Imaging System. Quantification of clotting dynamics was conducted on ImageJ by overlaying T-junction images and measuring the distance between clot apexes.

In vivo evaluation of tPA-FSN treatment in a rodent model of disseminated intravascular coagulation (DIC)

In a rat model of DIC, lipopolysaccharide (LPS) dissolved in 10 mL of sterile saline (30 mg/kg) was administered via the tail vein in male Sprague Dawley rats (~250g) over 4 hours. After DIC was induced, treatment was administered through 500 μL tail vein injections and allowed to circulate for 30 minutes. At least five animals were included in each treatment group. After treatment, blood was collected via a cardiac puncture for subsequent analysis in sodium citrate blood collection tubes (BD Vacutainer, Thermo Fisher Scientific), and organs were harvested and

weighed and cryopreserved and embedded in OCT compound for analysis and histology. DIC animals were compared to control animals (n=6). Cryosectioning utilized (Thermo Scientific HM525 NX) with 10 μm thickness. Staining was conducted on 4% paraformaldehyde-fixed sections. Three 10x images per tissue section were taken on an EVOS FL Auto Imaging System. Quantification of IHC images was conducted on ImageJ utilizing particle analysis to measure the number of microthrombi present in the tissue section. Quantification from three images per tissue section per animal were averaged for subsequent analysis.

Platelet count and platelet poor plasma (PPP) isolation was conducted from blood samples from each animal. Blood was first centrifuged at 150 G for 15 minutes, the top platelet rich plasma (PRP) layer separated, and 10% by volume additional ACD was added. The PRP was then centrifuged again at 900 G for 5 minutes to pellet the platelets, and the top layer now containing PPP was collected. Platelet count was performed using a hemocytometer with Tyrode's buffer (1 g/L $NaHCO_3$, 8.06 g/L NaCl, 1 g/L glucose, 0.216 g/L KCl, and 2.38 g/L HEPES). Cell counts were conducted in duplicate. The average of the two counts was used for subsequent analysis. For PPP samples, a fibrinogen ELISA and a D-Dimer ELISA were performed in duplicate for each animal. The average of the duplicate was used for subsequent analysis.

Evaluating coagulation parameters and bleeding outcomes following liver laceration in a rodent model of disseminated intravascular coagulation (DIC) with tPA-FSN treatment

Platelet count and platelet poor plasma (PPP) isolation was conducted from blood samples from each animal following injury. Platelet count (control n=6, vehicle n=7, DIC + saline n=7, DIC + FSN n=8, DIC + tPA-FSN n=5, DIC + tPA-CS-IgG n=6), and fibrinogen ELISA with PPP (control n=5, vehicle n=6, DIC + saline n=7, DIC + FSN n=7, DIC + tPA-FSN n=5, DIC + tPA-CS-IgG n=6) was also performed in duplicate. MSB and IHC staining was performed on 4%

paraformaldehyde-fixed wound sections for visualization of fibrin (UC45) (GeneTex) and platelets (SJ19-09) (Novus Biologicals). Images (10x magnification) were taken on an EVOS FL Auto Imaging System. Quantification of IHC images was conducted on ImageJ. For fibrin IHC, the integrated density was measured at the wound site for each animal (control n=5, vehicle n=5, DIC + saline n=6, DIC + FSN n=7, DIC + tPA-FSN n=5, DIC + tPA-CS-IgG n=6). For platelet IHC, particle analysis was utilized on ImageJ and for each animal (control n=6, vehicle n=5, DIC + saline n=7, DIC + FSN n=8, DIC + tPA-FSN n=5, DIC + tPA-CS-IgG n=6), an average particle count at the wound site was determined. Confocal microscopy was utilized to examine fibrin clot structure of PPP from animals after injury and quantify fiber density as described above where three images of each clot were taken and averaged for each animal (control n=6, vehicle n=7, DIC + saline n=7, DIC + FSN n=7, DIC + tPA-FSN n=5, DIC + tPA-CS-IgG n=6).

Evaluation of clotting dynamics of DIC patient plasma in Y-shaped microfluidic device under active coagulation

A custom-made Y-shaped microfluidic device was fabricated. Microchannels were prepared with standard soft lithography techniques. Photomasks were designed in AutoCAD (Autodesk Inc., San Rafael, CA) and prepared by FineLine Imaging (Colorado Springs, CO). SU-8 2050 (MicroChem Corp, Newton, MA) photoresist was spin coated in two layers on a 100mm silicon wafer and flood exposed under photomasks with a UV exposure system (OAI, Milpitas, CA) at a dosage of 370mJ/cm^2. Patterns were developed with SU-8 Developer (MicroChem Corp, Newton, MA) and rinsed with IPA. Resulting features were 234µm tall and 500µm wide. Uncured PDMS (Sylgard 184; Dow Corning, Midland, MI) was mixed at a 10:1 prepolymer-crosslinker ratio and poured onto the wafer to desiccate in a vacuum prior to curing at 60–80º in an oven for 45–60min. Cured PDMS was peeled from the wafer, sliced, and holes for 19 gauge Tygon tubing

were punched with a syringe tip. PDMS sections and glass slides were each cleaned with Scotch tape, acetone, and IPA, and sprayed with nitrogen gas. Glass and PDMS were then heated on a hot plate at 100ºC for at least 10min, followed by 2min cleaning in a tabletop oxygen plasma chamber (Harrick Plasma, Ithaca, NY). PDMS pieces were lightly pressed onto glass slides to allow bonding. Once assembled, a stationary fibrin clot boundary was formed at the top Y-junction with DIC patient plasma, 0.5 U/mL thrombin, and 0.05 mg/mL Alexa-Fluor 594 labeled fibrinogen (Thermo Fisher Scientific) for visualization in HEPES buffer. The stationary clot was allowed to polymerize for at least 30 minutes prior to experimentation. Then, a syringe pump was connected to the inlet tubing and an actively polymerizing solution was flowed into the device containing DIC patient plasma (from the same patient sample as the plasma used to form the stationary clot), 0.1 U/mL thrombin, and 0.05 mg/mL Alexa-Fluor 488 labeled fibrinogen in HEPES buffer. After the solution passed the stationary clot boundary site, the experiment continued for 20 minutes at wall shear rates of 10 s^{-1} with images taken (10x magnification on an EVOS FL Auto Imaging System) at the Y-junction and upstream inlet channel every 5 minutes. Endpoint images at the Y-junction and in the upstream inlet channel after 20 minutes are shown. Quantification of clotting dynamics was conducted on ImageJ by measuring clot growth in green at three positions of the stationary clot boundary at the Y-junction. Three trials were conducted with normal human plasma as a control. For each DIC patient's plasma sample (n=3 DIC patients), three trials were conducted with plasma alone in the flow solution, and three trials were conducted with plasma containing tPA-FSNs in the flow solution.

Tables

	Fibrinogen (mg/mL)	D-dimer (ng/mL)	Prothrombin Time (sec)	Prothrombin INR	Activated Partial Thromboplastin Time (sec)	Platelet Count (platelets/µL)
Normal Range	*200-400*	*<500*	*12-14*	*1*	*27-32*	*150,000-400,000*
DIC Patient 01	626	7,069	23.5	2.0	64.5	60,000
DIC Patient 02	148	58,071	25.9	2.3	31.5	-
DIC Patient 03	230	>100,000	21.4	1.8	-	47,000
Average +/- Standard Deviation	335 +/- 256	79,036 +/- 29,648	23.7 +/- 3.2	2.0 +/- 0.3	48 +/- 23.3	53,500 +/- 9,192

Supplemental Table 1: **Coagulation parameters from three DIC patient samples.** Parameters examined include fibrinogen, D-dimer, prothrombin time, prothrombin INR, activated partial thromboplastin time, and platelet count. Reference to normal ranges is shown and averages represent the average values from the three DIC patients.

		Control	Vehicle	DIC			
				Saline	FSN	tPA-FSN	tPA-CS-IgG
Microthrombi Presentation	Heart	0 ± 40 %	N/A	2209 ± 461 %; **	2857 ± 1778 %; ***	88 ± 124 %	1798 ± 1053 %, *
	Lung	0 ± 59 %	N/A	3774 ± 1494 %; ***	2963 ± 921 %; **	153 ± 157 %	2166 ± 2018 %; *
	Kidney	0 ± 67 %	N/A	1377 ± 736 %; ***	1154 ± 522 %; **	127 ± 272 %	924 ± 221 %; *
	Liver	0 ± 90 %	N/A	1174 ± 520 %; ****	1474 ± 505 %; ****	188 ± 241 %	208 ± 197 %
D-dimer		0 ± 49 %	N/A	939 ± 436 %; *	1288 ± 711 %; **	1498 ± 836 %; ***	949 ± 401 %; *
Fiber Density	Baseline	0 ± 53 %	N/A	-90 ± 7 %; **	-88 ± 9 %; **	-16 ± 57 %	-92 ± 4 %; **
	Post-bleed	0 ± 24 %	-46 ± 19 %; ***	-76 ± 15 %; ****	-78 ± 14 %; ****	-14 ± 28 %	-91 ± 7 %; ****
Fibrinogen	Baseline	0 ± 95 %	N/A	-72 ± 16 %	-73 ± 25 %	-72 ± 11 %	-64 ± 29 %
	Post-bleed	0 ± 83 %	25 ± 46 %	-61 ± 35 %	-30 ± 50 %	-83 ± 25 %; *	-85 ± 16 %; *
Platelets	Baseline	0 ± 40 %	N/A	-84 ± 6 %; ****	-61 ± 24 %; **	-15 ± 17 %	-72 ± 11 %; ***
	Post-bleed	0 ± 76 %	20 ± 75 %	-27 ± 32 %	-21 ± 24 %	49 ± 45 %	-2 ± 68 %
Blood Loss		0 ± 47 %	-9 ± 26 %	161 ± 123 %; **	160 ± 124 %; *	38 ± 96 %	229 ± 45 %; ***
Fibrin at wound		0 ± 42 %	-12 ± 39 %	-59 ± 10 %; *	-48 ± 15 %	17 ± 53 %	-46 ± 12 %
Platelets at wound		0 ± 55 %	10 ± 51 %	-76 ± 27 %; **	-71 ± 21 %; *	37 ± 64 %	-91 ± 9 %; **

Supplemental Table 2: Summary of results as a percent change of control. Results from *in vivo* experimentation in the DIC animal model, with and without injury, are summarized as a percent change of the control average for the corresponding parameter, showing differences between treatment groups. Data is presented as average +/- standard deviation. *p<0.05, **p<0.01, ***p<0.001, ****p<0.0001. Analyzed via a one-way analysis of variance (ANOVA) compared to controls with a Tukey's post hoc test using a 95% confidence interval.

Figures

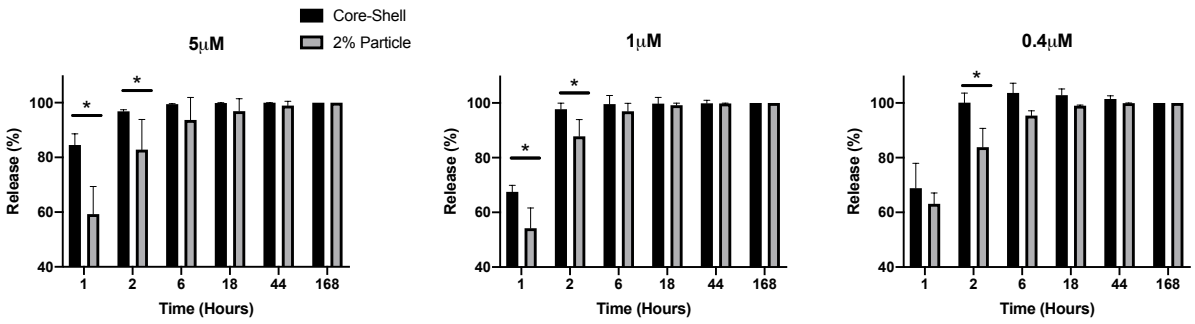

Supplemental Figure 1: Evaluation of release of drug mimic (dextran) from core-shell and 2% single layer particles. Release studies comparing core-shell to single-layer particle architecture with 5 μM, 1 μM, and 0.4 μM loading conditions of FITC-labelled 70kDa dextran (n=3 triplicate experiments). Data is presented as average +/- standard deviation. Release data was analyzed using multiple t-tests, two-tailed, correcting for multiple comparisons using the Holm-Sidak method with alpha=0.05. *p<0.05.

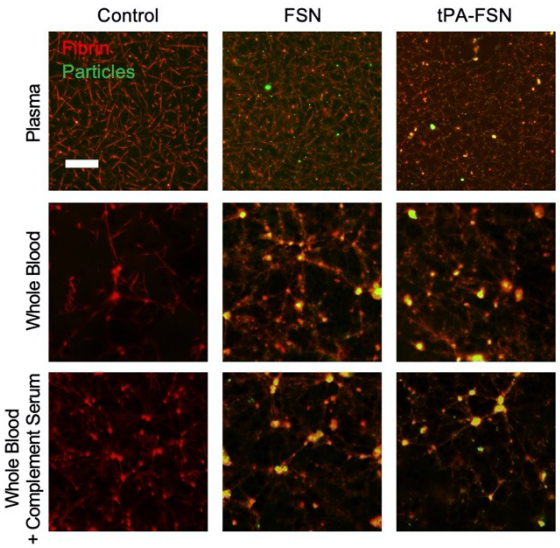

Supplemental Figure 2: **Particle behavior in plasma, whole blood, and whole blood with complement preserved serum.** Representative images are shown of FSNs and tPA-FSNs added to plasma, whole blood, and whole blood with 10% complement preserved serum to examine potential particle aggregation. Three clots for each condition were imaged where a final 2mg/mL concentration of particles was added and visualization of the particles (green) in fibrin (red) was observed. Scale bar is 20 μm.

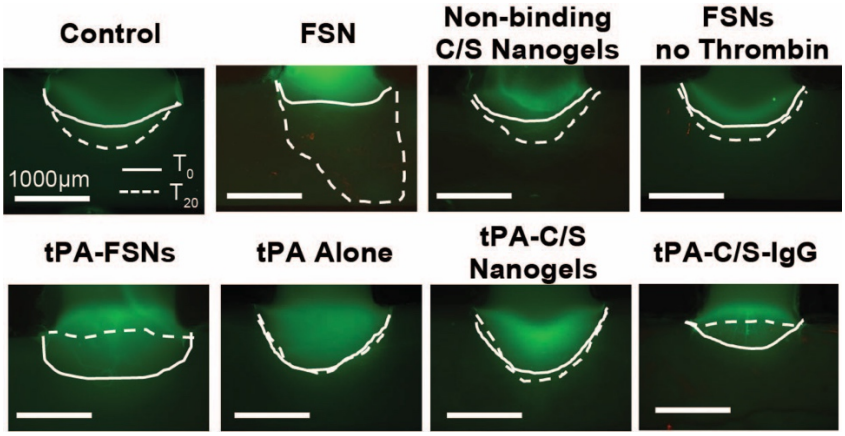

Supplemental Figure 3: ***In vitro*** **clotting under dynamic conditions in a T-junction PDMS fluidic device**. Representative images are shown of the stationary fibrin clot after a flow solution containing either fibrinogen and thrombin (control) (n=7), unloaded FSNs (n=4), non-binding core-shell nanogels (n=3), unloaded FSNs without thrombin and thus no active coagulation (n=3), tPA-FSNs (n=4), tPA alone (n=3), tPA-CS-IgG (n=3), or tPA loaded into non-binding core-shell nanogels (n=3) passed over the stationary clot boundary for 20 minutes. Solid line represents initial clot boundary and the dotted line represents the clot boundary after 20 minutes of flow at wall shear rate of $1s^{-1}$.

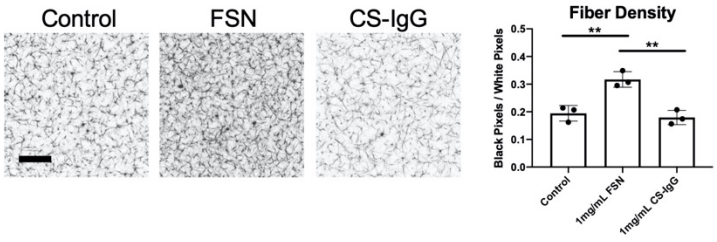

Supplemental Figure 4: Examination of clot structure with FSNs and CS-IgG particles. Clot microstructure visualized with clots made from purified fibrinogen with or without FSNs or CS-IgG particles through confocal microscopy. Corresponding fiber density quantification is shown (n=3 clots, 3 images per clot). Scale bar = 20 μm. Data is presented as average +/- standard deviation. **p<0.01. Analyzed via a one-way analysis of variance (ANOVA) with a Tukey's post hoc test using a 95% confidence interval.

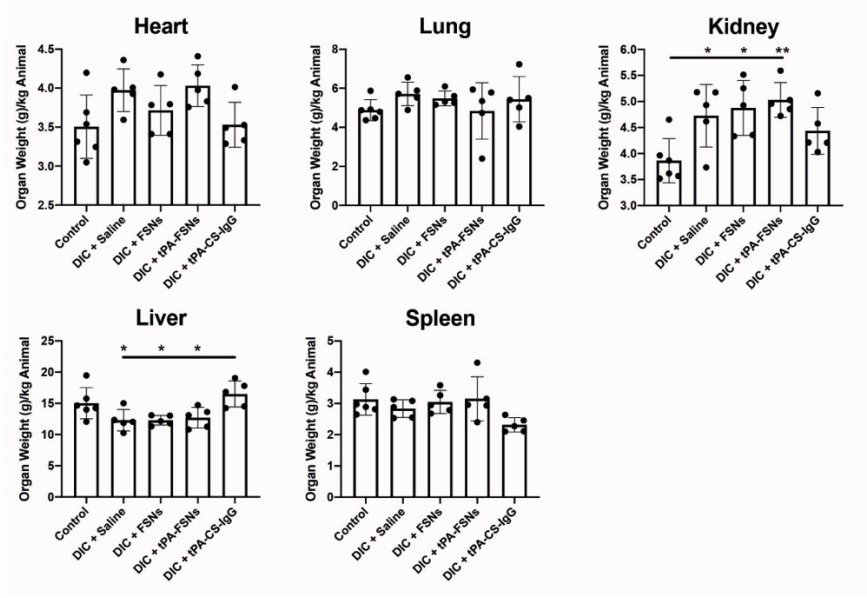

Supplemental Figure 5: **Organ weights in DIC rodent model**. Weights of the heart, lung, kidney, liver, and spleen from LPS-induced DIC animals compared to control animals are shown. Organs were harvested and weighed and normalized to animal weight (n=6 for control, n=5 for all other groups). Data is presented as average +/- standard deviation. Data sets were analyzed via a one-way analysis of variance (ANOVA) with a Tukey's post hoc test using a 95% confidence interval. *$p<0.05$, **$p<0.01$.

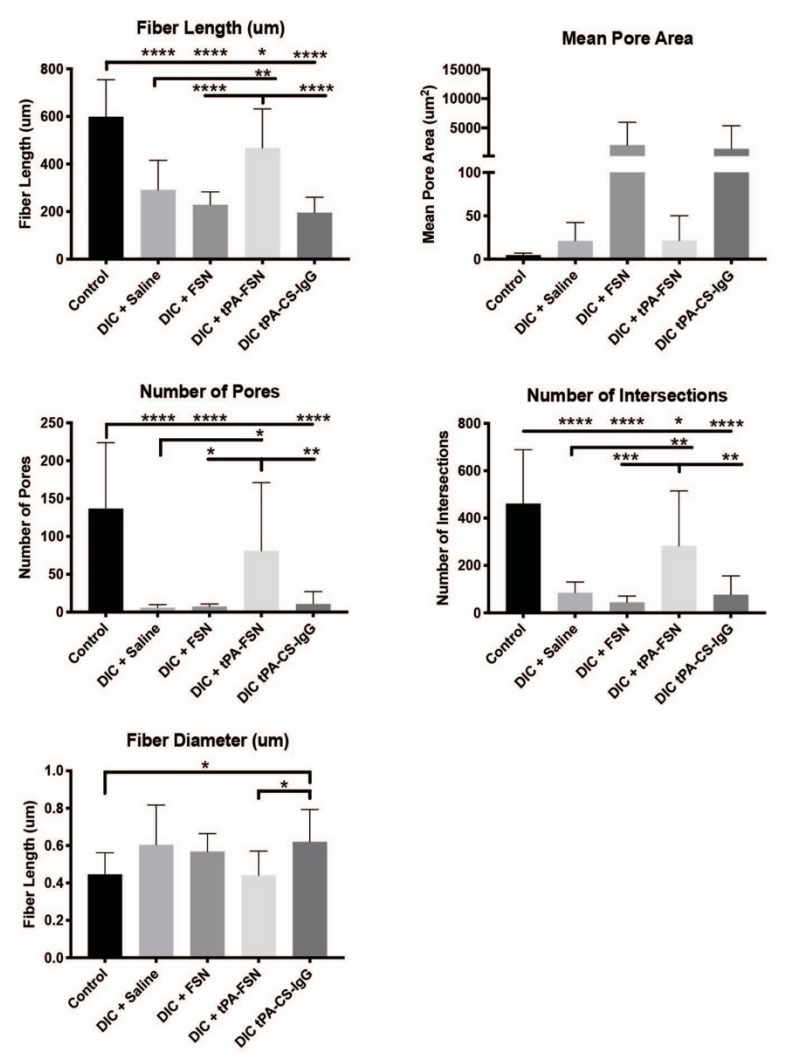

Supplemental Figure 6: **Quantification of clot structure from cryoSEM images taken of plasma clots formed from a rodent model of DIC**. Quantification of fiber length, mean pore area, number of pore, number of intersections, and fiber diameter from cryoSEM images where clot formation from control (n=6) and LPS-induced DIC animals treated with saline (n=5), FSNs (n=5), tPA-FSNs (n=5), or tPA-CS-IgG (n=5) were examined (n=2 or 3 images per animal). Data is presented as average +/- standard deviation. Data sets were analyzed via a one-way analysis of variance (ANOVA) with a Tukey's post hoc test using a 95% confidence interval. *$p<0.05$, **$p<0.01$, ****$p<0.0001$.

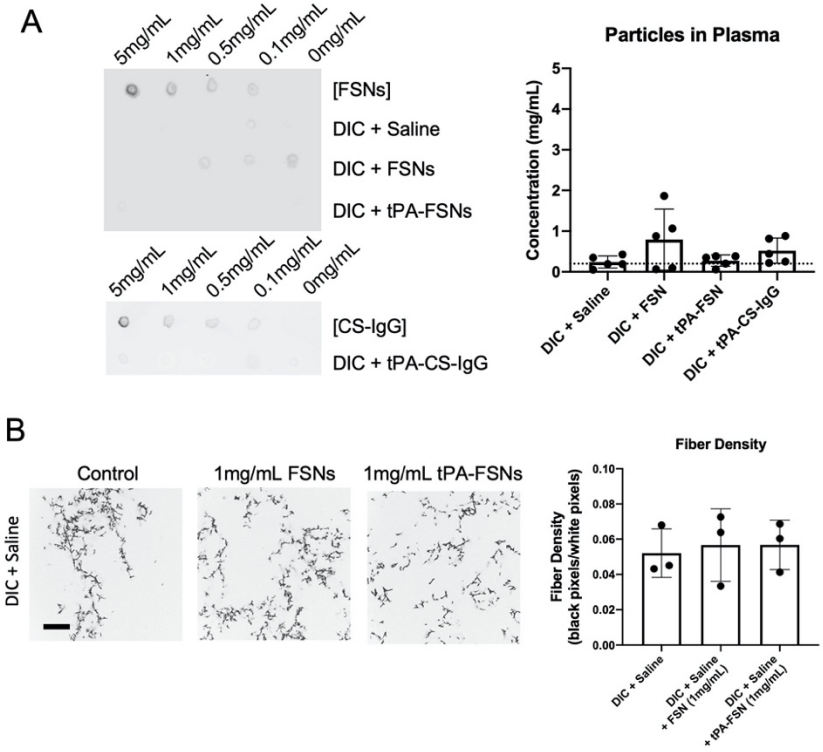

Supplemental Figure 7: *Ex vivo* analysis of residual particles in plasma from control and DIC animals. A dot blot analysis of residual particles in plasma and corresponding quantification from three averaged dot blots is shown (A). Exogenous addition of particles to DIC + Saline treated PPP to examine clot structure via confocal microscopy (B) and fiber density quantification. Data is presented as average +/- standard deviation. There are no significant differences between groups.

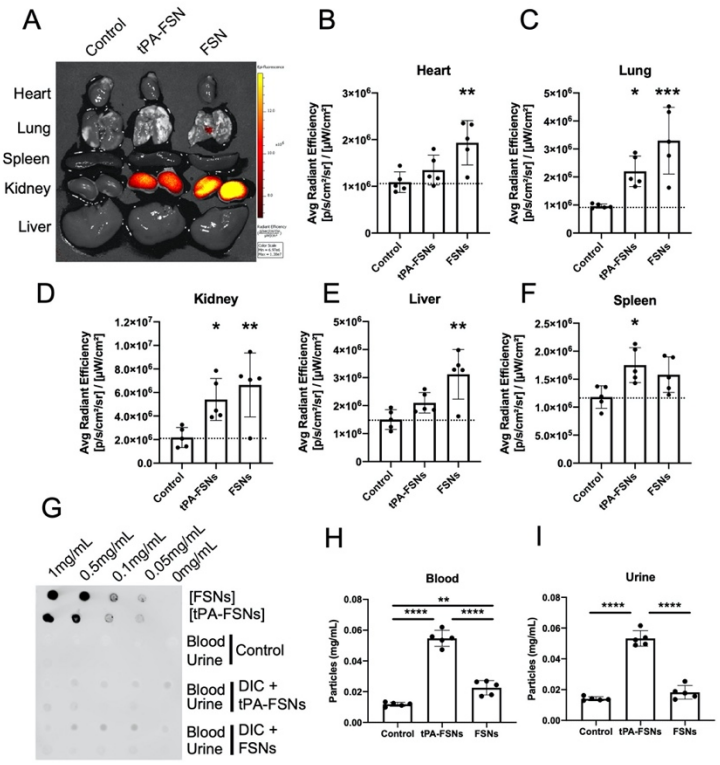

Supplemental Figure 8: Biodistribution of tPA-FSNs and FSNs in DIC animals after 30-minute circulation. IVIS Xenogen In Vivo Imager representative image (A) is shown and quantification of average radiant efficiency for each organ (B-F). Dot blot analysis (G) for distribution in the blood (H) and urine (I) is shown with corresponding quantification averaged from 3 dot blots. N=5 animals per group. Data is presented as average +/- standard deviation. Data sets were analyzed via a one-way analysis of variance (ANOVA) with a Tukey's post hoc test using a 95% confidence interval. *$p<0.05$, **$p<0.01$, ****$p<0.0001$.